Cell

EphB Signaling Directs Peripheral Nerve Regeneration through Sox2-Dependent Schwann Cell Sorting

Simona Parrinello,[1] Ilaria Napoli,[1] Sara Ribeiro,[1] Patrick Wingfield Digby,[1] Marina Fedorova,[1] David B. Parkinson,[2] Robin D.S. Doddrell,[2] Masanori Nakayama,[3] Ralf H. Adams,[3] and Alison C. Lloyd[1,*]

[1]MRC Laboratory for Molecular Cell Biology and the UCL Cancer Institute, University College London, Gower Street, London WC1E 6BT, UK

[2]Peninsula College of Medicine and Dentistry, University of Plymouth, Plymouth PL6 8BU, UK

[3]Department of Tissue Morphogenesis, Max Planck Institute for Molecular Biomedicine, and Faculty of Medicine, University of Münster, Münster D-48149, Germany

*Correspondence: alison.lloyd@ucl.ac.uk

DOI 10.1016/j.cell.2010.08.039

SUMMARY

The peripheral nervous system has astonishing regenerative capabilities in that cut nerves are able to reconnect and re-establish their function. Schwann cells are important players in this process, during which they dedifferentiate to a progenitor/stem cell and promote axonal regrowth. Here, we report that fibroblasts also play a key role. Upon nerve cut, ephrin-B/EphB2 signaling between fibroblasts and Schwann cells results in cell sorting, followed by directional collective cell migration of Schwann cells out of the nerve stumps to guide regrowing axons across the wound. Mechanistically, we find that cell-sorting downstream of EphB2 is mediated by the stemness factor Sox2 through N-cadherin relocalization to Schwann cell-cell contacts. In vivo, loss of EphB2 signaling impaired organized migration of Schwann cells, resulting in misdirected axonal regrowth. Our results identify a link between Ephs and Sox proteins, providing a mechanism by which progenitor cells can translate environmental cues to orchestrate the formation of new tissue.

INTRODUCTION

The peripheral nervous system (PNS) differs from the central nervous system (CNS) in that it is capable of remarkable regeneration even after severe injury. After an injury, both PNS and CNS axons distal to the lesion degenerate, but only PNS axons regrow and reconnect to their targets (Navarro, 2009; Zochodne, 2008). The distinct ability of peripheral nerves to regrow back to their targets hinges on the regenerative properties of its glia, the Schwann cells. Adult peripheral nerves lack a stem cell population to produce new glia. Instead, mature differentiated Schwann cells retain a high degree of plasticity throughout adult life and upon injury shed their myelin sheaths and dedifferentiate en masse to a progenitor/stem cell-like state (Kruger et al., 2002; Scherer and Salzer, 2001). Dedifferentiated Schwann cells are key to nerve repair for two main reasons. First, they can replenish lost or damaged tissue by proliferating. Second, they produce a favorable environment for axonal regrowth both by helping to clear myelin debris and by forming cellular conduits or corridors, known as bands of Buengner, that guide axons through the degenerated nerve stump and back to their targets (Zochodne, 2008).

Regeneration is particularly successful after crush injuries, because the basal lamina surrounding the axon/Schwann cell nerve unit is maintained, preserving the integrity of the original axonal paths and allowing highly efficient and accurate reinnervation (Nguyen et al., 2002). Regeneration also occurs after more severe injuries that significantly disrupt nerve structure, such as complete transection. However, the process is less efficient as transection presents several additional hurdles for successful repair (Nguyen et al., 2002). Upon cut, nerve stumps on either side of the cut retract, generating a gap, which must be bridged by new tissue; moreover, the regrowing axons from the proximal stump must travel through this newly formed tissue (referred to as the "nerve bridge") to reach the distal stump and ultimately their target organs (McDonald et al., 2006; Zochodne, 2008). While many studies have contributed to our understanding of how peripheral nerves repair after crush injuries, much less is understood about nerve regeneration after full transection. In particular, little is known about the mechanisms that control the formation and organization of new nerve tissue or how regrowing axons successfully negotiate the nerve bridge to rejoin the distal stump. Dissecting these events is key not only to the development of therapeutic strategies for the improvement of nerve regeneration but also to the understanding of basic principles governing the biology of stem cells and tissue development.

Ephrin/Ephs are a large family of receptor tyrosine kinases that function to convey positional information to cells (Lackmann and Boyd, 2008; Pasquale, 2008). During development, they direct cell migration, regulate tissue patterning, and help form tissue boundaries. In adulthood, they participate in the control of tissue homeostasis and, when aberrantly expressed, can contribute to

cancer development and progression. Eph receptors are subdivided into two classes: type A, which preferentially bind GPI-anchored ephrin-A ligands, and type B, which bind transmembrane B-type ephrins, although crosstalk between the two classes has been reported (Pasquale, 2008). Interaction between ephrin ligands and Eph receptors triggers complex bidirectional signaling, which modulates cell adhesion and repulsion, largely by reorganizing the actin cytoskeleton. A great deal is known about how ephrin/Eph signaling controls actin dynamics to cause rapid cell responses such as movement (Arvanitis and Davy, 2008). In contrast, very little is known about whether ephrin/Eph signaling can cause permanent changes in cell behavior by regulating gene expression, in spite of the potential importance of such mechanisms in development and regeneration.

Here, we show that ephrin-B/EphB signaling directs the early stages of peripheral nerve repair after transection. As Schwann cells emerge from both nerve stumps, they come into direct contact with fibroblasts, which accumulate at the injury site. In this region, ephrin-B/EphB2-mediated cell sorting of these two cell types orchestrates the collective cell migration of Schwann cells in the form of multicellular cords to guide axons across the injury site. The Schwann cell sorting downstream of EphB2 activation is mediated by Sox2-dependent relocalization of N-cadherin to contacts between the Schwann cells. Importantly, loss of EphB2 signaling in vivo in the context of a nerve cut impairs both the directional migration of Schwann cells and axonal regrowth.

RESULTS

Fibroblasts and Schwann Cells Sort at the Injury Site

To analyze the early stages of peripheral nerve repair after a severe injury, we initially performed a temporal analysis of Schwann cell and axonal behavior after a complete transection of the rat sciatic nerve (Figure 1A). We found that, by 2 days after the cut, the majority of transected nerves had spontaneously reconnected by formation of a nerve bridge, as judged by their macroscopic appearance (Figure S1 available online). We stained longitudinal frozen sections across the bridge site with antibodies against $p75^{NGFR}$ to label Schwann cells and against neurofilament to label the axons (whereas $p75^{NGFR}$ is only expressed in nonmyelinating Schwann cells in intact nerves [Figure 1A], its expression is induced in all Schwann cells upon dedifferentiation). As has previously been reported, we found that the nerve bridge between the two stumps was made up of cells other than Schwann cells, which are thought to be mainly inflammatory cells (see Hoechst staining in panels cut d2) (McDonald and Zochodne, 2003; Schröder et al., 1993). However, even at this early time point, dedifferentiated Schwann cells could be detected at the tips of both nerve stumps, whereas extensive axonal degeneration was only observed in the distal stump. By day 5, however, Schwann cells had collectively migrated into the nerve bridge from both stumps as discrete cell cords, which eventually met in the middle of the bridge. Regenerating axons from the proximal stump also entered the bridge at this time, closely following the migratory path of the Schwann cells. This comigration continued, until, by day 7,

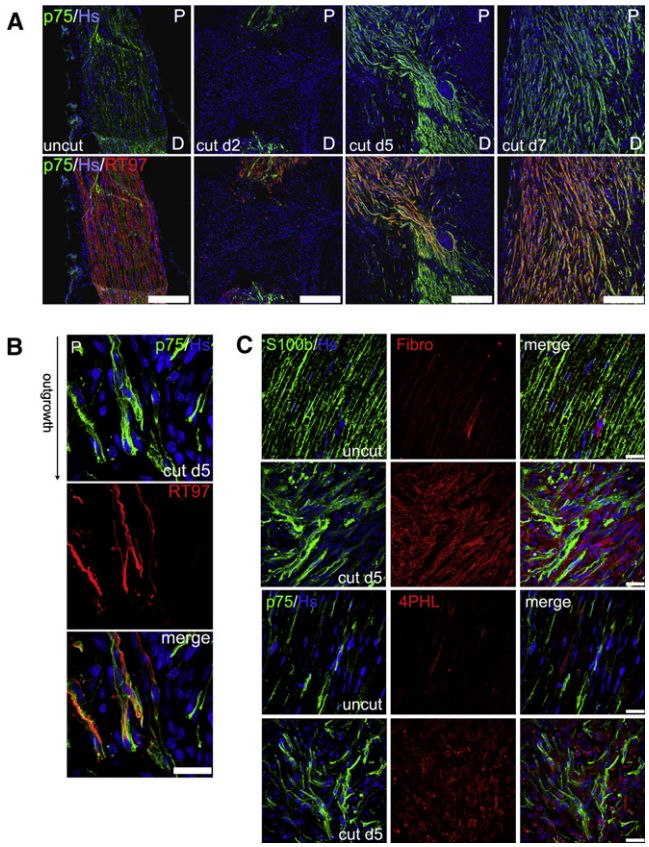

Figure 1. Fibroblasts Organize Schwann Cells into Cords that Lead Axons across the Injury Site after Nerve Cut

(A) Immunofluorescence staining for Schwann cell (SC) marker $p75^{NGFR}$ (green) and axonal neurofilament RT97 (red) of transverse sections of contralateral intact nerve (left panels, uncut) or cut nerve at time points after transection (middle and right panels, cut d2, d5 and d7). Nuclei were counterstained with Hoechst (Hs, blue). Scale bars represent 250 μm.

(B) Immunofluorescence staining for $p75^{NGFR}$ (green) and RT97 (red) of sections of nerve bridges 5 days after transection. The scale bar represents 25 μm.

(C) Immunofluorescence staining of sections of contralateral (uncut) and nerve bridges 5 days after transection (cut d5) for the following markers: S100β and $p75^{NGFR}$ for SC and fibronectin (Fibro) and 4-hydroxyprolyl (4PHL) for fibroblasts (Fb). Scale bars represent 25 μm.

See also Figure S1.

the whole width of the bridge was filled with Schwann cell cords and with axons, which had grown past the point of the initial transection and traveled into the distal stump. In agreement with previous studies (Chen et al., 2005; McDonald et al., 2006), closer examination of the cords at the leading edge of the migration front showed that Schwann cells apparently preceded the axons, suggesting that Schwann cell cords guide axonal regrowth across the injury site (Figure 1B).

Interestingly, the cords of migrating Schwann cells were surrounded by large numbers of other cells (Figure 1B, $p75^{NGFR}$-negative nuclei). As it has previously been reported that fibroblasts accumulate at sites of nerve injury (Morris et al., 1972; Schröder et al., 1993), we stained nerve bridges, 5 days after

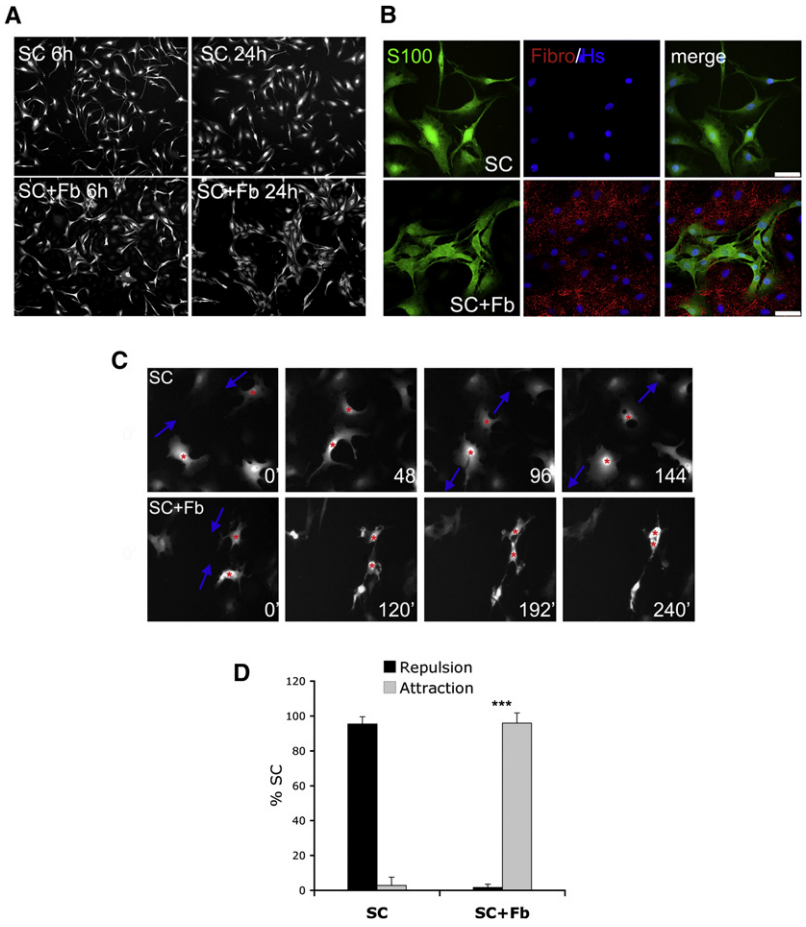

Figure 2. Fibroblasts Mediate Schwann Cell Sorting by Modifying Schwann Cell Behavior

(A) Immunofluorescence images of S100β-labeled SC cultured in the absence (SC) or presence (SC+Fb) of Fb, 6 and 24 hr after seeding.

(B) Immunofluorescence staining for S100β (S100) and fibronectin (Fibro) of SC monocultures (SC) or SC/Fb cocultures (SC+Fb). Scale bars represent 50 μm.

(C) Still images from time-lapse microscopy experiments of SC cultured alone (SC) or SC cocultured with Fb (SC+Fb). Shown is one example of SC repelling each other in the absence of Fb (top panels) and one example of SC adhering to one another in the presence of Fb (bottom panels). Numbers in white indicate elapsed time in minutes after plating.

(D) Quantification of SC behavior in movies described in (C). The bar graph represents the average number (±SD) of repulsive and adhesive events per condition. Three independent experiments were quantified by counting a minimum of 20 cells per video.

See also Figure S2 and Movies S1, S2, and S3.

cut, using two independent sets of fibroblasts markers (fibronectin and prolyl-4-hydroxylase, 4PHL), together with Schwann cell markers (S100β and $p75^{NGFR}$), to determine whether the cells surrounding the Schwann cell cords were fibroblasts (Figure 1C). This analysis showed that the two major cell types in the bridge at this point were Schwann cells and fibroblasts in close proximity to one another. Importantly, the two cell types did not appear to intermingle, but instead were clearly grouped into discrete clusters of cells of the same kind, possibly indicating a cell sorting event.

Fibroblasts Switch Schwann Cell Behavior in Culture to Induce Cell Sorting

To understand the cell and molecular events that control the interaction between Schwann cells and fibroblasts in nerve wounds, we cocultured primary rat Schwann cells and nerve fibroblasts. Both cell types were derived from P7 sciatic nerves and cultured according to previously established protocols, which allow the indefinite subculture of pure populations with intact cell-cycle checkpoints (Mathon et al., 2001). We seeded Schwann cells either on their own or on an equal number of fibroblasts; after 24 hr, we analyzed the behavior of the Schwann cells by immunostaining them with antibodies against S100β. As expected, when Schwann cells were plated alone, they were randomly distributed, and this did not change over time. In stark contrast, Schwann cells cultured with fibroblasts started to cluster together, and these Schwann cell clusters became larger by 24 hr after seeding (Figure 2A). Immunofluorescence analysis of the cocultures with both Schwann cell and fibroblast markers confirmed the sorting of the two cell types: similar to what we observed in vivo, Schwann cells and fibroblasts did not commingle, but instead organized themselves into mutually exclusive groups (Figure 2B). Similar results were obtained by coculturing Schwann cells and fibroblasts isolated from adult nerves (Figure S2), indicating that this is a general response of both young and adult cells. To better understand the cell behavior underlying the sorting of these cells, we performed time-lapse video microscopy on cultures of Schwann cells overexpressing GFP (SC-GFP)—either alone or seeded on fibroblasts. As shown in Figure 2C and Movies S1 and S2, SC-GFP cultured alone displayed contact inhibition of locomotion, which resulted in the cells separating from each other when they came into contact, a behavior predicted to result in an even distribution of cells. Strikingly, the presence of fibroblasts dramatically altered the behavior of the cells: instead of moving away, the Schwann cells adhered to one another, as quantified in Figure 2D. Additionally, videos of lower density cocultures of SC-GFP and fibroblasts (Movie S3) clearly showed that fibroblasts repelled Schwann cells, causing them to move away upon contact. These results indicate that the sorting of Schwann cells into clusters in the mixed cultures depends on two processes—the repulsion of Schwann cells by fibroblasts, coupled with a switch in Schwann cell behavior from repulsive to attractive.

Ephrin/Eph Signaling Mediates Schwann Cell/Fibroblast Sorting

We reasoned that fibroblasts might change Schwann cell behavior by secretion of a soluble signal, secretion of an

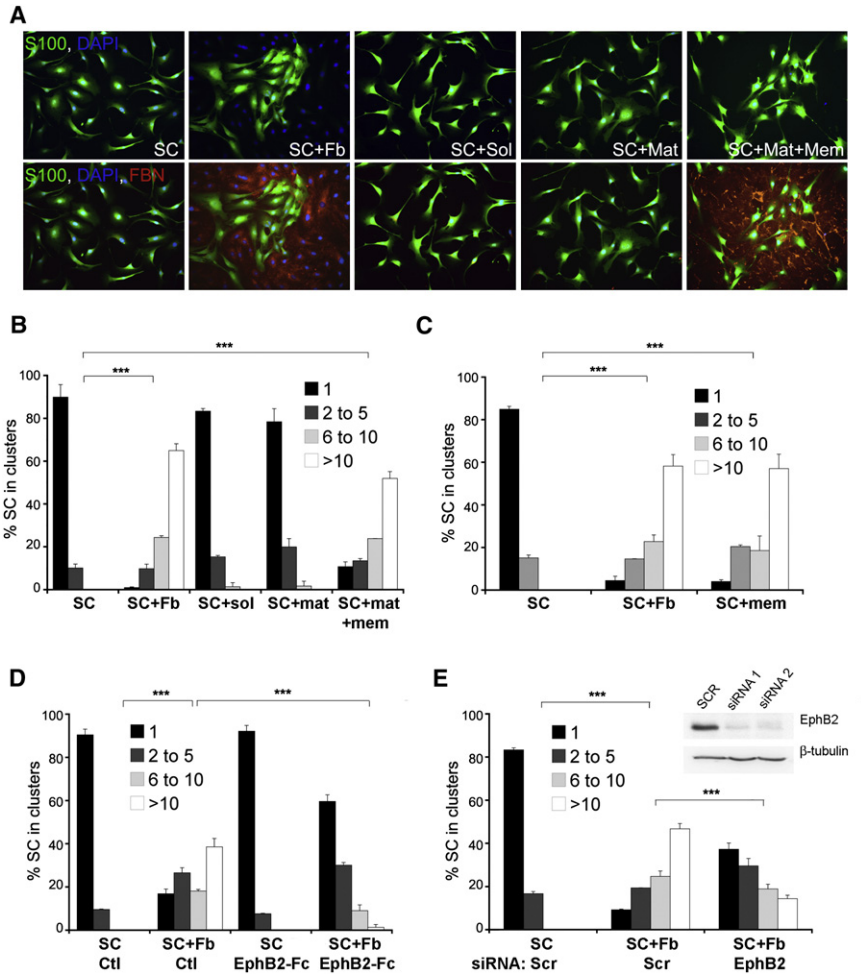

Figure 3. EphB2 Signaling Mediates Fibroblast-Induced Schwann Cell Sorting

(A) Immunofluorescence staining for S100β (S100) and fibronectin (FBN) of SC cultured alone (SC), in direct contact with Fb (SC+Fb), in the presence of Fb conditioned medium (SC+Sol), on Fb-secreted ECM (SC+Mat) or on Fb membranes and ECM (SC+Mat+Mem). Cells were fixed 24 hr after seeding.

(B) Quantification of SC clustering in the conditions depicted in (A). For this and all later experiments, a minimum of 200 cells per coverslip was counted across randomly selected fields of view, and the percentage of SC found in clusters of increasing size was calculated. Error bars indicate the SD across repeats of each condition (n = 2–3). Shown is a representative experiment of several that gave similar results. (*** $p < 0.001$).

(C) Quantification of SC clustering. Samples are SC monocultures (SC), direct cocultures of SC and Fb (SC+Fb) and SC monocultures in the presence of fibroblast membrane fractions (SC+mem).

(D) Quantification of clustering in SC cultures without (SC) or with Fb (SC+Fb) pretreated with control proteins (Ctl) or soluble recombinant EphB2-Fc fusion proteins (SC EphB2-Fc).

(E) Quantification of clustering of scr siRNA-treated SC in the absence (SC Scr) or presence of Fb (SC+Fb Scr) and EphB2 siRNA-treated SC cultured in the presence of Fb (SC+Fb EphB2). Western blots show efficacy of knockdown with two independent oligos.

See also Figure S3.

extracellular matrix (ECM) component, or direct cell-cell contact. To test the role of soluble factors, we separated the fibroblasts and Schwann cells in transwell plates (SC+Sol). To test the role of fibroblast-secreted ECM components, we plated Schwann cells on top of ECM left behind by fibroblasts after they were removed using nonenzymatic cell dissociation buffers (SC+Mat). Finally, to test the role of cell-contact-dependent signaling, we treated confluent fibroblasts with water for 1 hr to kill the cells but preserve their membranes and cultured Schwann cells on top of them. As this treatment also preserved fibroblast-secreted ECM components, we refer to this condition as Schwann cell on matrix and membranes (SC+Mat+Mem). We analyzed Schwann cell sorting in these three conditions using immunofluorescence staining for S100β and fibronectin and quantified Schwann cell clustering (Figures 3A and 3B). Whereas neither the soluble nor the insoluble secreted fraction of fibroblast cultures induced Schwann cell clustering, the insoluble and membrane fractions in combination produced clustering comparable to that produced by intact fibroblasts. This result suggested that fibroblasts induce sorting through direct cell-cell contact. To confirm this directly and rule out a cooperative role for the ECM, we purified fibroblast membranes by fractionation and added these to Schwann cell cultures. As shown in Figure 3C, the fibroblast-membrane fraction alone was sufficient to cluster Schwann cells, confirming that direct contact between Schwann cells and fibroblasts mediates Schwann cell sorting.

Ephrin/Eph signaling has been shown to be a major mediator of cell-contact-dependent cell sorting. To address whether it has a role in our system, we stained our cultures with an antibody that recognizes most phosphorylated Eph receptors and found high levels of phospho-Eph staining specifically in the Schwann cell clusters formed in the presence of fibroblasts (Figure S3A). We then treated Schwann cell cultures with preclustered soluble recombinant class A or class B ephrins and found that all three B-type ephrins induced significant Schwann cell clustering, whereas A-type ephrins did not (Figure S3B), suggesting that a B-type ephrin on nerve fibroblasts induces sorting. To confirm that the sorting behavior was solely mediated by ephrin-B signaling, independently of other membrane components of the fibroblasts, we overexpressed ephrin-B2 in MDA-MB-435 breast cancer cells, which normally do not express ephrin-B2 (Figure S3C) (Noren et al., 2006). Consistent with the results obtained with soluble ephrin-B ligands, coculture of Schwann cells with MDA-MB-435-ephrin-B2 cells, but not MDA-MB-435-GFP controls, induced Schwann cell clustering, indicating

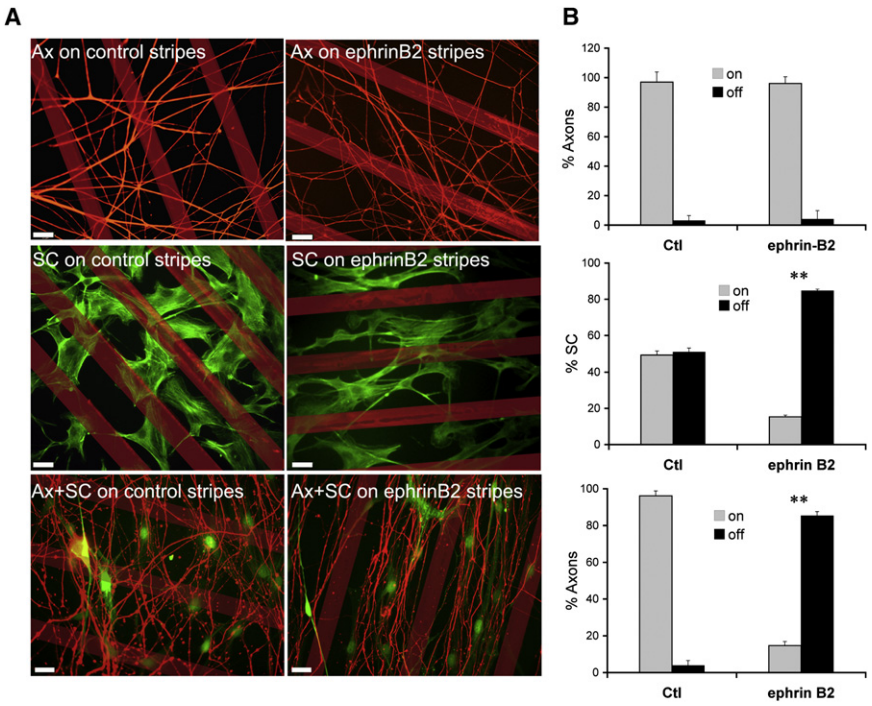

Figure 4. Schwann Cell Organization Affects Axonal Outgrowth

Fluorescence images (A) and quantification (B) of SC and axonal individual and cocultures in stripe assays.

(A) Representative images of DRGs and SC cultured alone (top and middle panels) or together (bottom panels) on control or ephrin-B2-Fc stripes. SC were labeled with phalloidin or visualized by GFP fluorescence (middle and bottom panels respectively), and axons were stained with neurofilament. Scale bars represent 25 μm.

(B) Effects of ephrin-B2 on SC positioning and axonal outgrowth were quantified by counting the number of SC and axons on and off the stripes. A minimum of 200 cells and axons per coverslip was scored in duplicate per condition. Error bars denote the SD across repeats (** $p < 0.005$).

that ephrin-B2 is sufficient to induce Schwann cell sorting (Figures S3C and S3D).

To determine which *Eph* and *efn* genes Schwann cells and nerve fibroblasts express, we performed quantitative RT-PCR (Table S1). We found that both Schwann cells and fibroblasts expressed EphB receptors and ephrin-B ligands; however, the expression levels were very different between the two cell types. Specifically, fibroblasts expressed much higher levels of ephrin-B2 ligand, which was low or undetectable in Schwann cells. In contrast, Schwann cells expressed higher levels of EphB receptors than fibroblasts, with the most significant difference found for EphB2 expression (Figure S3E).

To test whether EphB2 mediates Schwann cell sorting, we took two parallel approaches: (1) we inhibited EphB2 signaling by preincubating fibroblast cultures with soluble recombinant EphB2-Fc fusion proteins prior to seeding Schwann cells and (2) we used two independent small interfering RNA (siRNA) oligos to knock down EphB2 in Schwann cells, prior to coculturing them with fibroblasts. In both cases, reduction of EphB2 signaling strongly inhibited Schwann cell clustering in the presence of fibroblasts (Figures 3D and 3E and Figure S3F). Importantly, the sorting defect of EphB2 knockdown cells was rescued by concomitant transient transfection of siRNA-insensitive mouse *EphB2*, confirming the specificity of the EphB2 phenotype (Figure S3G). Thus, ephrin-B/EphB2 signaling between fibroblasts and Schwann cells mediates cell sorting.

Ephrin-B Signaling Results in Directional Axonal Outgrowth

It is known that ephrin/Eph signaling can promote the directional movement of cells by constraining migrating cells to specific areas through active repulsion. This has been shown, for example, to help guide the migration of neural crest cells and axon growth cones during development (Kuriyama and Mayor, 2008; Lackmann and Boyd, 2008). Both the collective migration of Schwann cells and the regrowth of axons after nerve transection are also directional in that the majority of cords and axons are parallel to one another and migrate along the long axis of the nerve stumps (see Figure 1A). We therefore asked whether EphB2/ephrin-B signaling might be responsible for directing organized Schwann cell and/or axonal migration. To do this, we performed stripe assays using microcontact printing (von Philipsborn et al., 2006). We generated lines of preclustered recombinant ephrin-B2 or control protein and seeded Schwann cells at low density or explanted postnatal rat DRGs onto the stripes. In the presence of NGF, axonal processes migrate out of the DRG core, mimicking axonal regrowth after injury. Remarkably, Schwann cells cultured on ephrin-B2 stripes, but not on control stripes, accumulated between the stripes, forming parallel lines of cells reminiscent of the Schwann cell cords observed in transected nerves in vivo. In contrast, axonal outgrowth from DRG explants was indistinguishable on control and ephrin-B2 stripes, with most axons crossing the stripes at multiple points, indicating that DRG axons are not repelled by ephrin-B2 (Figures 4A and 4B). However, when DRGs were explanted onto SC-GFP cells, which had previously been grown for 4 days on ephrin-B2 stripes, the axons grew out onto the Schwann cells, between the stripes, to form axon fascicles (Figures 4A and 4B). These data demonstrate that ephrin signaling can direct axonal outgrowth by modulating Schwann cell behavior.

Fibroblast-Mediated Sorting Involves N-Cadherin Relocalization to Schwann Cell Contacts

We have shown that EphB2 stimulation triggers Schwann cell clustering, in part by promoting Schwann cell adhesion, suggesting a possible change in cell-surface adhesion molecules. Both N- and E-cadherins are expressed by Schwann cells and

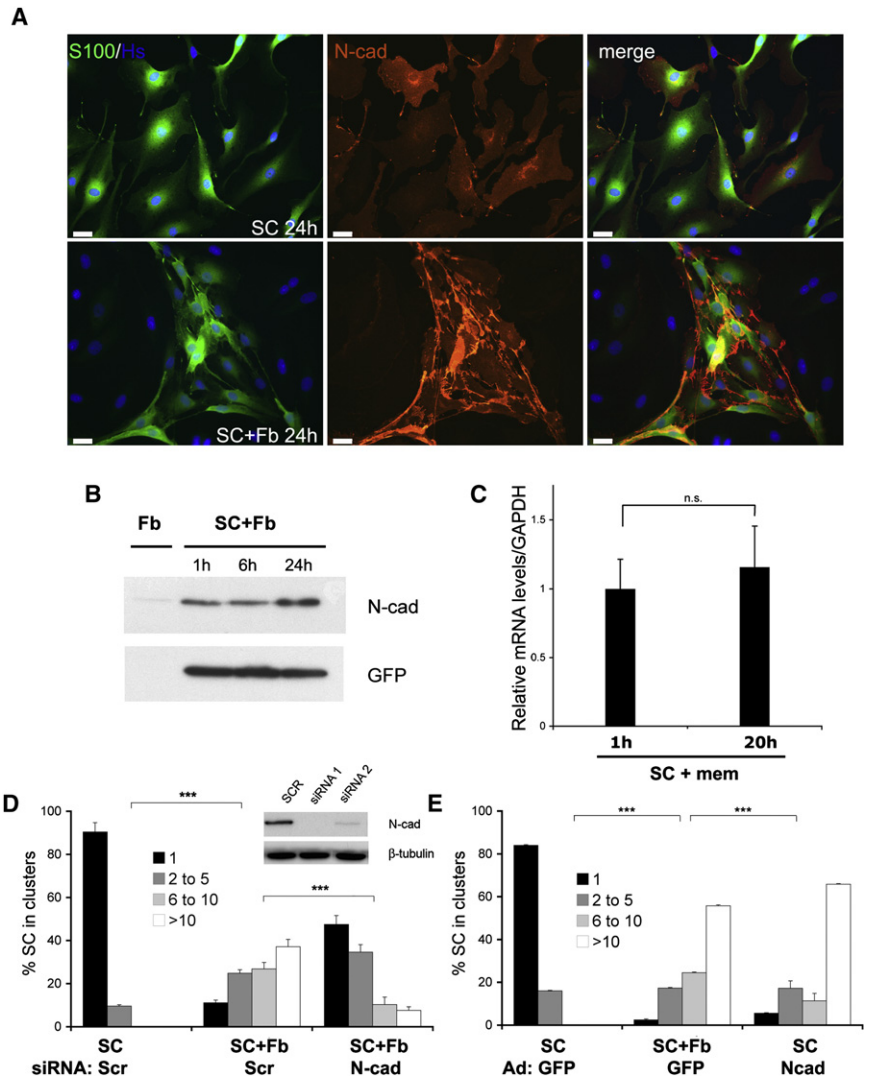

Figure 5. N-Cadherin Relocalization to Cell Junctions Mediates Cell Sorting

(A) Representative immunofluorescence images of Schwann cells cultured on their own (SC) or with fibroblasts (Fb) for 24 hr and stained for N-cad (red) and S100β (green). Scale bars represent 25 μm.

(B) Western blot analysis of total protein lysates from fibroblast membranes used as control or GFP expressing Schwann cells cultured on fibroblast membranes for the indicated times. GFP levels were used as loading control.

(C) Quantitative RT-PCR analysis of N-cad mRNA levels in Schwann cells cultured on fibroblast membranes for the indicated times. The average of three independent experiments is shown ± SEM.

(D) Quantification of clustering of scr siRNA-treated Schwann cells in the absence (SC Scr) or presence of fibroblasts (SC+Fb Scr) and of N-cad knockdown Schwann cells cultured in the presence of fibroblasts (SC+Fb N-cad). Western blots show efficacy of N-cadherin knockdown with two independent oligos. The mean is shown as ± SD.

(E) Quantification of clustering of Schwann cells infected with adenoviral vectors encoding control GFP or N-cadherin in the absence of fibroblasts. See also Figure S4.

have been reported to have roles in cell sorting (Halbleib and Nelson, 2006). N-cadherin (N-cad) is expressed during development, is downregulated in adult nerves, and is re-expressed in dedifferentiated Schwann cells after nerve injury; in contrast, E-cadherin (E-cad) is present only in differentiated Schwann cells (Crawford et al., 2008; Wanner et al., 2006a). When we stained Schwann cells cultured alone or in the presence of fibroblasts with antibodies against E- and N-cad, we could not detect E-cad on the Schwann cells (data not shown). In contrast, N-cad was readily detectable in Schwann cell monocultures with expression detected throughout the cytoplasm and at the membrane. However, the pattern of N-cad expression dramatically changed in the Schwann cell/fibroblast cocultures with a progressive increase in levels at cell-cell contacts as shown in Figure 5A and Figure S4A and quantified in Figure S4B; western analysis of N-cad levels showed that the shift in N-cad distribution was accompanied by an increase in protein levels at 24 hr after seeding, when cell sorting was fully established (Figure 5B). We obtained similar results when we treated Schwann cells with soluble ephrin-B2 (Figures S4C and S4D). Importantly, the late increase in N-cad protein was not accompanied by a rise in its messenger RNA (mRNA), as judged by quantitative RT-PCR (Figure 5C), suggesting that the increase may have resulted from post-transcriptional changes in protein levels. Together, these results suggest that relocalization of N-cad to junctions in the absence of changes in expression is sufficient to initiate Schwann cell sorting. However, we cannot rule out the possibility that the late increase in N-cad levels might be required for the stabilization and maintenance of sorting.

To test whether the redistribution of N-cad was necessary for the cell sorting, we used two independent siRNA oligos to knock down N-cad in Schwann cells and scored Schwann cell clustering in the presence of fibroblasts (Figure 5D and Figure S3F). Clustering was strongly reduced in N-cad-deficient cells, suggesting that N-cad is a critical mediator of the sorting process. Moreover, rescue experiments in which siRNA-resistant N-cad was overexpressed in N-cad knockdown Schwann cells confirmed the specificity of the knockdown (Figure S4E). To determine whether higher levels of N-cad at cell junctions were sufficient to induce clustering, we mimicked the relocalization by overexpressing N-cad using adenoviral vectors, which results in elevated N-cad levels throughout the cell (data not shown). Remarkably, N-cad overexpression in Schwann cells induced large clusters in the absence of fibroblasts (Figure 5E). Thus, EphB2 signaling in Schwann cells induces cell sorting, at

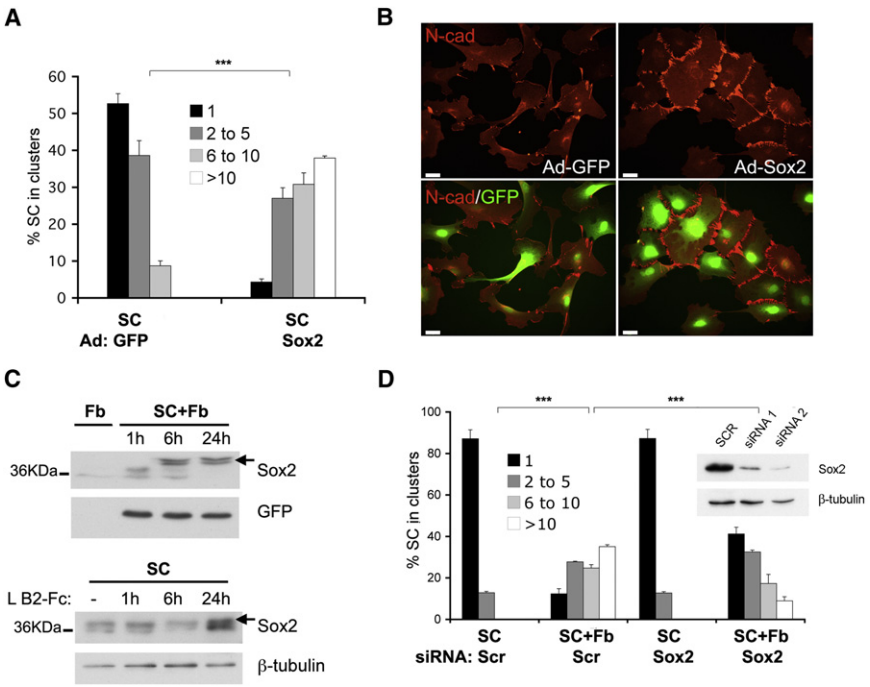

Figure 6. EphB2 Signals through Sox2 to Induce N-Cadherin Remodeling

(A) Quantification of clustering of Schwann cell cultures infected with adenoviruses encoding GFP or Sox2-GFP.

(B) Representative immunofluorescence images of GFP- and Sox2-GFP-overexpressing Schwann cells stained for N-cadherin (red). Endogenous GFP fluorescence is also shown. Scale bars represent 25 μm.

(C) Top: western analysis of lysates of GFP-overexpressing Schwann cells cultured on fibroblast membranes for indicated times. GFP levels were used for loading control. Bottom: western analysis of lysates from Schwann cells treated with preclustered recombinant ephrin-B2 for indicated time intervals.

(D) Quantification of clustering of scr siRNA-treated and Sox2 knockdown Schwann cells cultured in the absence (SC Scr; SC Sox2) or presence (SC+Fb Scr; SC+Fb Sox2) of fibroblasts. Insert shows western analysis of Sox2 knockdown and loading control (β-tubulin).

See also Figure S5.

least in part by causing the redistribution of N-cad to cell-cell contacts.

EphB2-Induced Relocalization of N-Cadherin Is Sox2 Dependent

EphB signaling was recently shown to mediate cell sorting of colorectal cancer cells in an E-cadherin-dependent manner, suggesting that crosstalk between Ephs and cadherins may be a general mechanism for directing cell sorting (Cortina et al., 2007). However, the mechanism of the crosstalk and the sorting process itself are poorly understood. Cell sorting is a complex process, requiring cell recognition, followed by cell movement, an extensive process of fine-tuning, culminating in the establishment of cell groups through the stabilization of cell-cell contacts (Tepass et al., 2002). Moreover, once established, cell and tissue boundaries both in culture and in vivo are maintained, suggesting that sorting requires long-term modifications in cell behavior and thus is likely to involve changes in gene expression. The transcription factor Sox2 plays a pivotal role in the development and maintenance of some stem and progenitor cells (Chambers and Tomlinson, 2009). Consistent with these functions, it was recently shown that Sox2 is expressed in progenitor Schwann cells in developing nerves and is re-expressed in dedifferentiated Schwann cells, where it is thought to promote proliferation and suppress differentiation (Le et al., 2005). While studying the function of Sox2 in Schwann cells, we observed that overexpression of Sox2 induced the formation of cell clusters, suggesting that it might be involved in ephrin B-mediated Schwann cell sorting. To test this idea, we overexpressed Sox2 in subconfluent Schwann cells using an adenoviral vector, and quantified clustering. As shown in Figure 6A, overexpression of Sox2 was sufficient to cluster Schwann cells, mimicking the effect of fibroblasts. Moreover, like fibroblast-induced Schwann cell clusters, Sox2-induced clusters displayed an increase in junctional N-cad staining (Figure 6B and Figure S5A), without an increase in total N-cad protein levels or mRNA (Figures S5B and S5C). To test the dependence of Sox2-mediated clustering on N-cad-based cell-cell junctions, we infected Schwann cell cultures with adeno-GPP or adeno-Sox2 viruses in normal or low Ca^{2+} media, in which the extracellular domains of cadherins cannot homodimerize to form junctions (Letourneau et al., 1991). We found that Sox2-mediated clustering was abolished in low Ca^{2+} culture conditions, confirming that Sox2 promotes Schwann cell clustering by inducing the formation of N-cad junctions (Figure S5D). To test whether Sox2 might be a target of EphB2, we measured Sox2 protein levels in Schwann cells cultured on fibroblasts membranes and Schwann cells treated with soluble ephrin-B2 ligands by western blotting. In both cases, Sox2 increased in amount and also increased in apparent size, suggesting a posttranslational modification (Figure 6C). These observations suggest that EphB2 might induce cell sorting by modifying gene expression via the transcription factor Sox2. Consistent with this suggestion, treatment of fibroblast-Schwann cell cocultures with the transcriptional inhibitor actinomycin D blocked the relocalization of N-cad (data not shown). To address whether Sox2 is necessary for fibroblast-induced Schwann cell sorting, we knocked down Sox2 by siRNA in Schwann cells using two independent oligos prior to culturing them with fibroblasts and found that clustering was greatly reduced in the Sox2-deficient cells (Figure 6D and Figure S3F). Importantly, the phenotype of rat Sox2-deficient cells was rescued by adenoviral re-expression of siRNA-resistant mouse Sox2 (Figure S5E), confirming that the sorting is Sox2-dependent. Together, our results suggest the following

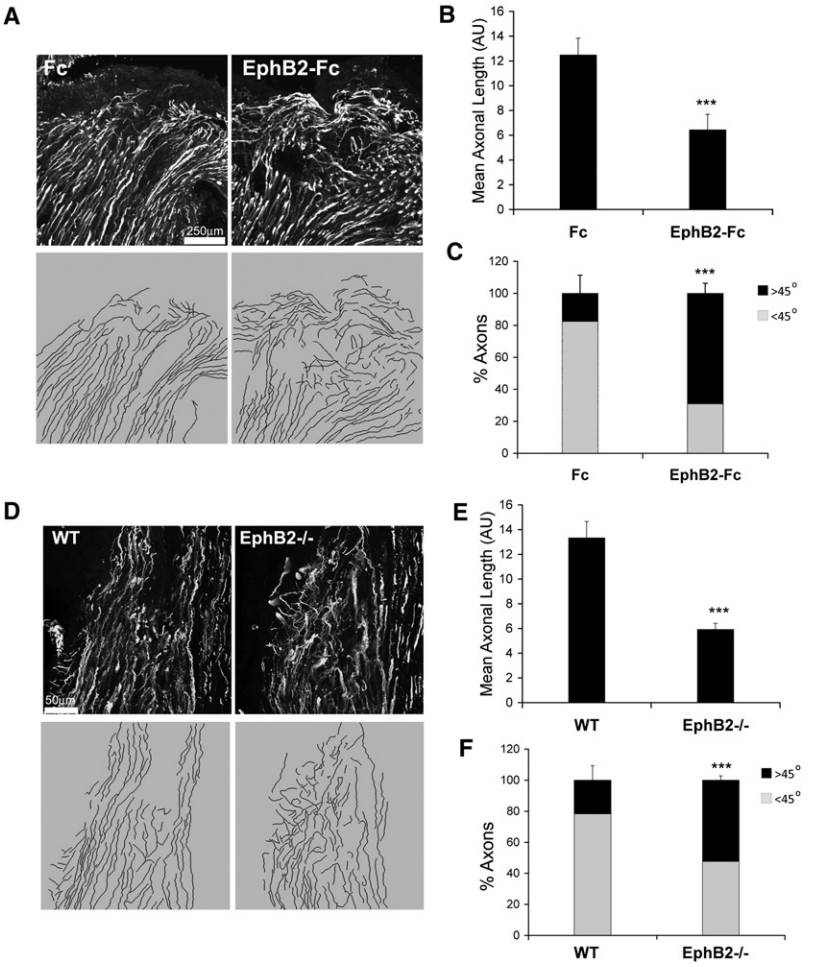

Figure 7. EphB2 Directs Early Nerve Regeneration In Vivo

(A) Representative immunofluorescence staining for axonal RT97 of sections of proximal nerve stumps of cut nerves 4 days after half transection. Control proteins (Fc) or recombinant EphB2 (EphB2-Fc) were delivered to the cut nerve region via osmotic pumps. The bottom panels show axonal tracings of images shown in the top panels obtained with NeuronJ.

(B) Quantification of axonal length as a measure of complexity. Values represent average length of axons per animal group. Error bars represent the SD, n = 7 (*** $p < 0.001$).

(C) Quantification of axonal growth angles to long axis of the nerves. Shown is the average of the percentage of axons at angles <45° or >45° per animal group. Error bars represent the SD, n = 7 (*** $p < 0.001$).

(D) Representative immunofluorescence staining for axonal neurofilament of sections of proximal nerve stumps of cut wild-type (WT) and *EphB2*$^{-/-}$ mice nerves 4 days after half transection and axonal tracings of images shown in (E) obtained with NeuronJ (bottom).

(E and F) Quantification of WT and *EphB2*$^{-/-}$ samples as in (C) and (D). n = 5 (*** $p < 0.001$).

See also Figure S6.

mechanism: activation of EphB2 receptor on Schwann cells by ephrin-B on fibroblasts leads to the modification and stabilization of Sox2 protein in Schwann cells, resulting in the relocalization of N-cad to the cell-cell contact regions of these cells, which in turn promotes their sorting. To validate this sequence of events, we performed two complementary experiments: we treated Sox2 knockdown cells with soluble ephrin-B2 ligands and overexpressed Sox2 in EphB2 knockdown cells. As shown in Figures S5F and S5G, we found that Sox2 loss impaired ephrin-B2-dependent clustering, while Sox2 overexpression rescued the phenotype of EphB2-deficient Schwann cells, confirming that EphB2 receptor acts upstream of Sox2. Importantly, these findings identify a link between Eph signaling and Sox2, providing a mechanism by which ephrin/Eph signaling can elicit long-term transcriptional changes.

EphB2 Signaling Mediates Directional Collective Cell Migration In Vivo

We have shown that Schwann cells and fibroblasts are in direct contact and undergo cell sorting in nerve wounds, suggesting that the same molecular mechanisms that mediate Schwann cell/fibroblast cell sorting in culture might be important for orchestrating the changes in tissue structure seen in vivo. To test this possibility more directly, we immunostained frozen sections of cut nerve, on day 5 after transection (or contralateral control nerves), using antibodies against EphB2, N-cad, or Sox2, together with Schwann cell-specific markers (Figures S6A–S6C). Strikingly, we found that dedifferentiated Schwann cell cords in the nerve bridge, but not differentiated Schwann cells expressed all three proteins. The staining however revealed distinct patterns of expression along the nerve. EphB2 and Sox2 were present throughout the distal stump and in the most distal portion of the proximal stump (as expected for Sox2; Le et al. [2005]), consistent with the switch-on of these genes as part of the dedifferentiation program of the Schwann cells. In contrast and consistent with our results in culture, N-cad staining was restricted to cords in the bridge region, which is where the Schwann cells come into direct contact with the fibroblasts.

We next used two approaches to investigate the role of EphB2 in nerve regeneration in vivo: we inhibited EphB2 signaling pharmacologically in rats and examined nerve regeneration in *EphB2*$^{-/-}$ mice (Henkemeyer et al., 1996). For the former approach, we employed mini osmotic pumps to deliver inhibitory EphB2-Fc fusion proteins (or control Fc proteins) to the injury site of cut sciatic nerves. In both types of experiments, we cut halfway across the nerve in order to keep the stumps in close proximity, thereby minimizing the variability in the speed of regeneration. Four days after surgery, we immunostained frozen sections of the nerves and analyzed axonal outgrowth from the proximal stump (Figure 7). In all nerves, we found an almost complete overlap between Schwann cell cords and axons (Figure S6D) and therefore used axonal regrowth as a readout of Schwann cell behavior. Remarkably, both EphB2-Fc-treated

and *EphB2*$^{-/-}$ nerves displayed a similar phenotype, which was markedly different from Fc-treated or wild-type nerves (Figures 7A and 7D). In control nerves, axonal outgrowth was regular, mostly parallel to the uncut region and remained within the plane of the section. In contrast, in nerves that lacked EphB2 signaling, regrowth appeared less organized, with axons growing in many different directions and often disappearing out of the plane of the section. We quantified this behavior by measuring axonal length and the angles of axonal outgrowth with respect to the long axis of the nerves (Figures 7B, 7C, 7E, and 7F). Compared to control nerves, EphB2-deficient nerves presented significantly shorter and more fragmented axons, which more often grew at angles greater than 45° from the uncut region. We conclude that EphB2 signaling directs the migration of Schwann cells and axons during early nerve regeneration in vivo.

DISCUSSION

The development of a multicellular organism relies on the coordinated and mass movement of groups of specialized cells. The mechanisms that control these processes have been extensively studied, and much insight has been gained into how positional cues orchestrate complex developmental processes such as tissue patterning and boundary formation (Kuriyama and Mayor, 2008; Tepass et al., 2002). What is less well understood is how cell reorganization and movement may be reinitiated in adult organisms to repair tissues after a major injury. In some regenerative tissues, it appears that repair, after injury in the adult, recapitulates developmental processes (Chargé and Rudnicki, 2004; Deschaseaux et al., 2009). However, in many cases, the cell types responsible for repair are distinct from their developmental counterparts and the positional cues are no longer present, suggesting that different mechanisms must also be involved. Peripheral nerve regeneration after severe injury is an example of de novo postdevelopmental tissue formation. For successful nerve regeneration, migrating Schwann cells and regrowing axons must both find their way through the bridge region to close the nerve gap and integrate within the preestablished geometry of the adult tissue (McDonald et al., 2006). Most of the mechanisms whereby tissue organization is established within the newly forming nerve bridge to promote reinnervation of the distal stump are unknown. Here, we show that ephrin/Eph signaling is a major mediator of this process.

We find that, after severe nerve trauma, large numbers of fibroblasts accumulate at the injury site. It is well established that fibroblasts play a key role in wound healing by secreting new ECM and promoting tissue contraction, both of which contribute to scar formation. Additionally, they are thought to promote angiogenesis and inflammation by secreting proangiogenic and proinflammatory cytokines (Sorrell and Caplan, 2009). We now identify an additional role for fibroblasts in wound repair—initiating tissue reconstruction by orchestrating directed cell migration. By recapitulating this behavior in vitro by the coculture of Schwann cells and nerve fibroblasts, we show that this was the result of fibroblasts triggering a highly efficient switch in the behavior of the Schwann cells—from repulsion to adhesion. This switch is induced by the activation of EphB2 receptors on Schwann cells by ephrin-B on fibroblasts. We show that a similar segregation of EphB2^{+} Schwann cells from fibroblasts occurs in the nerve bridge in vivo, where the cells come into direct contact with each other. These findings suggest that, through EphB2/ephrin signaling, fibroblasts induce the Schwann cells to migrate through the bridge as compact groups, or cords. Interestingly, a study on CNS repair observed activation of Eph signaling at astrocyte/fibroblast borders during glial scar formation, suggesting that the re-establishment of tissue organization through Eph signaling might be a general function of fibroblasts in wound healing (Bundesen et al., 2003).

Our work also confirms that regenerating axons rely on their interaction with Schwann cells for directional guidance. In agreement with previous studies, we find that Schwann cells appear to precede regrowing axons in the nerve bridge (Chen et al., 2005; McDonald et al., 2006). Moreover, Schwann cells appear to be required to guide axons across the bridge to the distal stump, as disruption of Schwann cell interactions by loss of EphB2 results in aberrant axonal regrowth. This is in agreement with our in vitro observations that DRG axons fail to respond to ephrin-B2 but are indirectly organized by tracks of Schwann cells that form between stripes of ephrin-B2. These findings are also consistent with a recent report that inhibition of Schwann cell proliferation and migration in the nerve bridge using a mitotic inhibitor resulted in misdirected axons (Chen et al., 2005). The mechanisms that guide regenerating axons after nerve injury therefore seem to be distinct from those that guide axons in the developing PNS. In development, axons have been shown to lead glial migration during limb formation and to respond directly to guidance cues, including ephrin-B signaling (Gilmour et al., 2002; Luria et al., 2008; Wang and Anderson, 1997). However, it has also been reported that during the final stages of limb innervation, as developing axons approach their targets, the growth cones become almost completely surrounded by Schwann cell progenitors (Wanner et al., 2006b). Moreover, several lines of evidence from in vivo studies suggest that glial cells, while dispensable for initial pathfinding, are necessary for late axonal fasciculation and targeting, suggesting that at these later stages of development, Schwann cells can influence axonal growth (Gilmour et al., 2002; Morris et al., 1999; Nguyen et al., 2002). Thus, regeneration processes might be partially recapitulating late nerve development. It would therefore be of great interest to explore whether ephrin-B/EphB signaling plays a role in the migration of Schwann cell progenitors during limb innervation.

It is commonly thought that Eph signaling elicits short-term changes in cell behavior, mainly by modulating the actin cytoskeleton. Our findings suggest that it can also elicit longer-term changes through the transcription factor Sox2. Intriguingly, EphA4 receptor has been shown to directly activate the transcription factor Stat3 in skeletal muscle, suggesting that modulation of transcription might be a common property of Ephs (Lai et al., 2004) and important for ephrin-directed, long term cell responses. We also show that Sox2-dependent, EphB2-mediated Schwann cell sorting is induced by the redistribution of N-cadherin to cell-cell junctions and that this process is dependent on transcription. Although we have not yet identified the Sox2 target genes responsible, our unpublished observations suggest that multiple changes in gene expression might be

involved. Whatever the mechanisms, this change in N-cadherin distribution is likely to promote the regeneration process by maintaining migrating Schwann cells in groups, thereby providing a favorable substrate for axonal regrowth (Scherer and Salzer, 2001).

Sox2 is best known for its central role in the maintenance of embryonic stem cell self-renewal and pluripotency (Chambers and Tomlinson, 2009). It has also been shown to be one of the transcription factors that can help reprogram somatic cells to become induced pluripotent stem cells (Chambers and Tomlinson, 2009; Takahashi and Yamanaka, 2006). Our work uncovers a novel function of Sox2 in progenitor cells—the coordination of cell movement and tissue patterning by eliciting long-term changes in cell behavior in response to extracellular positional cues. Given the widespread expression of ephrins, Eph receptors, and Sox transcription factors during development, the regulation of Sox proteins by ephrin/Eph signaling may be a general mechanism regulating progenitor cells during the formation of tissues and organs.

EXPERIMENTAL PROCEDURES

Cell Culture

Primary rat Schwann cells and fibroblasts were cultured from P7 animals as previously reported (Mathon et al., 2001). For cocultures, fibroblasts were seeded at 7.5×10^4 per cm^2 on PLL-laminin in fibroblast medium. The next day, Schwann cells were added at the same density in a 1:5 mixture of Schwann cell medium and defined medium as described (Parrinello et al., 2008). Cultures were analyzed 24 hr later unless otherwise specified. Clustering was quantified by counting the number of Schwann cells found in groups of 1, 2–5, 6–10 or >10 cells. Adenoviral infections were performed as reported (Parrinello et al., 2008). For modifications of coculture protocols, see the Extended Experimental Procedures.

Immunofluorescence, Immunohistochemistry and Western Blotting

Contralateral or cut sciatic nerves at d2, 4, 5, 7, 9, and 10 posttransection were analyzed; only relevant stages are shown. Nerves were processed and stained as reported (Wanner et al., 2006a). Sections for immunostaining (8–15 μm) or for quantification of axonal outgrowth (40–60 μm) were cut with a cryostat (Leica). For EphB2 staining on sections, signal was amplified using a TSA kit (Invitrogen). Western blotting and immunostaining were performed as previously described (Parrinello et al., 2008). For description of antibodies, see the Extended Experimental Procedures.

Recombinant Protein Treatments and Stripe Assays

Recombinant ephrin-Fc fusions (R&D systems) were preclustered with anti-human Fc antibodies (Jackson Laboratory) at a 2:1 molar ratio and added to Schwann cells at a final concentration of 8 μg/ml. For inhibition studies, EphB2-Fc fusion proteins (R&D systems) were added at 10 μg/ml (culture) and 200 μg/ml (in vivo). Fc fragments or anti-Fc antibodies alone were used as negative controls with similar results. Stripes of preclustered ephrin-B2 or control proteins (10–20 μg/ml) were stamped onto PLL-coated coverslips generated by microcontact printing and later visualized with fluorescently labeled anti-Fc antibodies as reported (von Philipsborn et al., 2006). After laminin coating, Schwann cells or DRGs were seeded. For Schwann cell/DRG coculture experiments, DRGs were plated onto pre-established GFP-expressing Schwann cells in the presence of 1 μg/ml aphidicolin to prevent outgrowth of endogenous glia.

Statistics

For all clustering experiments, statistical analysis was performed by Fisher's exact test for rxq contingency tables. Significance was calculated with the Wilcoxon rank-sum test for all qPCR data and with the Student's t test for all other experiments.

Surgeries

All animal work was carried out in accordance to the guidelines and regulations of the Home Office. Adult (6- to 8-week-old) Sprague-Dawley male rats and 4- to 6-week-old *EphB2*$^{-/-}$ mice and littermate controls (Henkemeyer et al., 1996) were used for all experiments. For immunohistochemical analysis, left sciatic nerves were exposed, under general anesthesia in aseptic conditions, and transected at midthigh. For inhibition studies, half of the nerve trunk was cut, and the wounded region was inserted into a silicone tube connected laterally at a 90° angle to a smaller caliber tube to which a catheter was attached. A mini osmotic pump (1007D; Alzet) implanted subcutaneously above the left buttock was then used to deliver control or inhibitor proteins to the cut site through the catheter. Wounds were closed using surgical clips. Four days after surgery, nerves were collected and processed for immunohistochemistry. *EphB2*$^{-/-}$ mice wounding experiments were performed in the same way except that no tubing was used and wounds were reclosed immediately after half transection. For details of quantification, see the Extended Experimental Procedures.

SUPPLEMENTAL INFORMATION

Supplemental Information includes Extended Experimental Procedures, six figures, three tables, and three movies and can be found with this article online at doi:10.1016/j.cell.2010.08.039.

ACKNOWLEDGMENTS

S.P. is a Royal Society D.H. Research Fellow. This work was supported by a Cancer Research UK program and an Association for International Cancer Research project grant. We thank C.D. Nobes for advice and M. Raff and B. Baum for critical reading of the manuscript, M. Herlyn, J. Milbrandt, E. Battle, and D. Wilkinson for constructs and G. Parrinello, A. Mira, and J. Kriston-Vizi for statistics.

Received: March 11, 2010
Revised: July 15, 2010
Accepted: August 9, 2010
Published online: September 23, 2010

REFERENCES

Arvanitis, D., and Davy, A. (2008). Eph/ephrin signaling: networks. Genes Dev. *22*, 416–429.

Bundesen, L.Q., Scheel, T.A., Bregman, B.S., and Kromer, L.F. (2003). Ephrin-B2 and EphB2 regulation of astrocyte-meningeal fibroblast interactions in response to spinal cord lesions in adult rats. J. Neurosci. *23*, 7789–7800.

Chambers, I., and Tomlinson, S.R. (2009). The transcriptional foundation of pluripotency. Development *136*, 2311–2322.

Chargé, S.B., and Rudnicki, M.A. (2004). Cellular and molecular regulation of muscle regeneration. Physiol. Rev. *84*, 209–238.

Chen, Y.Y., McDonald, D., Cheng, C., Magnowski, B., Durand, J., and Zochodne, D.W. (2005). Axon and Schwann cell partnership during nerve regrowth. J. Neuropathol. Exp. Neurol. *64*, 613–622.

Cortina, C., Palomo-Ponce, S., Iglesias, M., Fernández-Masip, J.L., Vivancos, A., Whissell, G., Humà, M., Peiró, N., Gallego, L., Jonkheer, S., et al. (2007). EphB-ephrin-B interactions suppress colorectal cancer progression by compartmentalizing tumor cells. Nat. Genet. *39*, 1376–1383.

Crawford, A.T., Desai, D., Gokina, P., Basak, S., and Kim, H.A. (2008). E-cadherin expression in postnatal Schwann cells is regulated by the cAMP-dependent protein kinase a pathway. Glia *56*, 1637–1647.

Deschaseaux, F., Sensébé, L., and Heymann, D. (2009). Mechanisms of bone repair and regeneration. Trends Mol. Med. *15*, 417–429.

Gilmour, D.T., Maischein, H.M., and Nüsslein-Volhard, C. (2002). Migration and function of a glial subtype in the vertebrate peripheral nervous system. Neuron *34*, 577–588.

Halbleib, J.M., and Nelson, W.J. (2006). Cadherins in development: cell adhesion, sorting, and tissue morphogenesis. Genes Dev. *20*, 3199–3214.

Henkemeyer, M., Orioli, D., Henderson, J.T., Saxton, T.M., Roder, J., Pawson, T., and Klein, R. (1996). Nuk controls pathfinding of commissural axons in the mammalian central nervous system. Cell *86*, 35–46.

Kruger, G.M., Mosher, J.T., Bixby, S., Joseph, N., Iwashita, T., and Morrison, S.J. (2002). Neural crest stem cells persist in the adult gut but undergo changes in self-renewal, neuronal subtype potential, and factor responsiveness. Neuron *35*, 657–669.

Kuriyama, S., and Mayor, R. (2008). Molecular analysis of neural crest migration. Philos. Trans. R. Soc. Lond. B Biol. Sci. *363*, 1349–1362.

Lackmann, M., and Boyd, A.W. (2008). Eph, a protein family coming of age: more confusion, insight, or complexity? Sci. Signal. *1*, re2.

Lai, K.O., Chen, Y., Po, H.M., Lok, K.C., Gong, K., and Ip, N.Y. (2004). Identification of the Jak/Stat proteins as novel downstream targets of EphA4 signaling in muscle: implications in the regulation of acetylcholinesterase expression. J. Biol. Chem. *279*, 13383–13392.

Le, N., Nagarajan, R., Wang, J.Y., Araki, T., Schmidt, R.E., and Milbrandt, J. (2005). Analysis of congenital hypomyelinating Egr2Lo/Lo nerves identifies Sox2 as an inhibitor of Schwann cell differentiation and myelination. Proc. Natl. Acad. Sci. USA *102*, 2596–2601.

Letourneau, P.C., Roche, F.K., Shattuck, T.A., Lemmon, V., and Takeichi, M. (1991). Interactions of Schwann cells with neurites and with other Schwann cells involve the calcium-dependent adhesion molecule, N-cadherin. J. Neurobiol. *22*, 707–720.

Luria, V., Krawchuk, D., Jessell, T.M., Laufer, E., and Kania, A. (2008). Specification of motor axon trajectory by ephrin-B:EphB signaling: symmetrical control of axonal patterning in the developing limb. Neuron *60*, 1039–1053.

Mathon, N.F., Malcolm, D.S., Harrisingh, M.C., Cheng, L., and Lloyd, A.C. (2001). Lack of replicative senescence in normal rodent glia. Science *291*, 872–875.

McDonald, D.S., and Zochodne, D.W. (2003). An injectable nerve regeneration chamber for studies of unstable soluble growth factors. J. Neurosci. Methods *122*, 171–178.

McDonald, D., Cheng, C., Chen, Y., and Zochodne, D. (2006). Early events of peripheral nerve regeneration. Neuron Glia Biol. *2*, 139–147.

Morris, J.H., Hudson, A.R., and Weddell, G. (1972). A study of degeneration and regeneration in the divided rat sciatic nerve based on electron microscopy. IV. Changes in fascicular microtopography, perineurium and endoneurial fibroblasts. Z. Zellforsch. Mikrosk. Anat. *124*, 165–203.

Morris, J.K., Lin, W., Hauser, C., Marchuk, Y., Getman, D., and Lee, K.F. (1999). Rescue of the cardiac defect in ErbB2 mutant mice reveals essential roles of ErbB2 in peripheral nervous system development. Neuron *23*, 273–283.

Navarro, X. (2009). Chapter 27: Neural plasticity after nerve injury and regeneration. Int. Rev. Neurobiol. *87*, 483–505.

Nguyen, Q.T., Sanes, J.R., and Lichtman, J.W. (2002). Pre-existing pathways promote precise projection patterns. Nat. Neurosci. *5*, 861–867.

Noren, N.K., Foos, G., Hauser, C.A., and Pasquale, E.B. (2006). The EphB4 receptor suppresses breast cancer cell tumorigenicity through an Abl-Crk pathway. Nat. Cell Biol. *8*, 815–825.

Parrinello, S., Noon, L.A., Harrisingh, M.C., Digby, P.W., Rosenberg, L.H., Cremona, C.A., Echave, P., Flanagan, A.M., Parada, L.F., and Lloyd, A.C. (2008). NF1 loss disrupts Schwann cell-axonal interactions: a novel role for semaphorin 4F. Genes Dev. *22*, 3335–3348.

Pasquale, E.B. (2008). Eph-ephrin bidirectional signaling in physiology and disease. Cell *133*, 38–52.

Scherer, S.S., and Salzer, J.L. (2001). Axon-Schwann Cell Interactions during Peripheral Nerve Degeneration and Regeneration (Oxford: Oxford University Press).

Schröder, J.M., May, R., and Weis, J. (1993). Perineurial cells are the first to traverse gaps of peripheral nerves in silicone tubes. Clin. Neurol. Neurosurg. Suppl. *95*, S78–S83.

Sorrell, J.M., and Caplan, A.I. (2009). Fibroblasts-a diverse population at the center of it all. Int. Rev. Cell. Mol. Biol. *276*, 161–214.

Takahashi, K., and Yamanaka, S. (2006). Induction of pluripotent stem cells from mouse embryonic and adult fibroblast cultures by defined factors. Cell *126*, 663–676.

Tepass, U., Godt, D., and Winklbauer, R. (2002). Cell sorting in animal development: signalling and adhesive mechanisms in the formation of tissue boundaries. Curr. Opin. Genet. Dev. *12*, 572–582.

von Philipsborn, A.C., Lang, S., Bernard, A., Loeschinger, J., David, C., Lehnert, D., Bastmeyer, M., and Bonhoeffer, F. (2006). Microcontact printing of axon guidance molecules for generation of graded patterns. Nat. Protoc. *1*, 1322–1328.

Wang, H.U., and Anderson, D.J. (1997). Eph family transmembrane ligands can mediate repulsive guidance of trunk neural crest migration and motor axon outgrowth. Neuron *18*, 383–396.

Wanner, I.B., Guerra, N.K., Mahoney, J., Kumar, A., Wood, P.M., Mirsky, R., and Jessen, K.R. (2006a). Role of N-cadherin in Schwann cell precursors of growing nerves. Glia *54*, 439–459.

Wanner, I.B., Mahoney, J., Jessen, K.R., Wood, P.M., Bates, M., and Bunge, M.B. (2006b). Invariant mantling of growth cones by Schwann cell precursors characterize growing peripheral nerve fronts. Glia *54*, 424–438.

Zochodne, D.W. (2008). Neurobiology of Peripheral Nerve Regeneration, First Edition (New York: Cambridge University Press).

Cell

EXTENDED EXPERIMENTAL PROCEDURES

Antibodies

Primary antibodies for Western blotting and immunofluorescence analysis were: anti-RT97 (kind gift of J. Woods), anti-neurofilament (Abcam), anti-S100β (DAKO), anti-$p75^{NGFR}$ (Chemicon), anti-fibronectin (Sigma), anti-prolyl-4-hydroxylase β (Acris), N-cadherin (BD transduction labs), anti-p-Eph (kind gift of K. Nobes), anti-EphB2 (R&D systems), anti-Sox2 (kind gift of M. Wegner).

Co-culture Modifications

Effects of fibroblast soluble, matrix and matrix+membrane fractions on Schwann cell clustering were assessed as follows. Schwann cells were seeded on the bottom chamber of a culture dish containing a transwell insert (Falcon) onto which confluent fibroblasts were seeded, or onto matrices prepared by culturing fibroblasts to confluency and then removing them from the dish with non-enzymatic cell dissociation buffers (Invitrogen) or lysing them with H2O for 1h at 37°C. For membrane fractionation experiments, purified membrane fractions were prepared as reported (Kapfhammer et al., 2007) and were added to Schwann cell cultures for 24-48h.

Quantification of Axonal Outgrowth In Vivo

To quantify axonal outgrowth after nerve cut in the absence or presence of recombinant EphB2, the whole sciatic nerve was sectioned, stained and examined. Representative sections, which were parallel to the length of the nerve as judged by the positioning of the uncut region, were further quantified for axonal length using the ImageJ macro NeuronJ (Meijering et al., 2004). Additionally, the number of axons growing at an angle smaller or greater than 45° to the nerve axis were counted for each sample. A total of 9 control-treated and 10-EphB2-treated animals were analyzed. Of the EphB2 group, 7 showed a clear phenotype, one could not be analyzed because of incorrect sectioning angle and 2 had no phenotype, most likely due to malfunctioning of the pump and/or delivery system. Of the control group, one nerve could not be scored for the same reasons as above. The remaining 8 animals showed no disruption in axonal outgrowth and had a phenotype indistinguishable from untreated nerves. For the experiments in mouse, 5 animals of each group were analyzed as above. All knock-out animals showed a strong phenotype.

Quantification of N-Cadherin Immunofluorescence

Junctional N-cadherin levels were quantified using Metamorph 6.0 software. Pixel intensity was measured at cell-cell contacts and normalized to contact area. A minimum of 80 junctions across multiple randomly selected images was quantified. The average of the total pixel intensity of 4-6 images was calculated per condition.

siRNA and qPCR

RNA silencing and quantitative RT-PCR were performed as reported previously (Parrinello et al., 2008). See also Table S2 and Table S3.

siRNA Rescue Experiments

All siRNA oligos used for rescue experiments were specific for rat sequences (see table, oligo 1). For N-cadherin and Sox2 rescue experiments, human and mouse genes respectively were delivered using adenoviral vectors 36 hr after siRNA transfection. 18 hr post-infection Schwann cells were co-cultured with fibroblasts for 6-8 hr. For EphB2 rescue experiments RNA oligos and plasmids were delivered simultaneously using attractene reagent (QIAGEN) according to the manufacturers instructions. A GFP-encoding vector was also co-transfected to label transfected cells. 36 hr later cells were co-cultured with fibroblasts for 18 hr and only GFP positive cells were scored. Efficacy of knockdown and overexpression of relevant genes was confirmed by Western blotting and qPCR (not shown).

SUPPLEMENTAL REFERENCES

Kapfhammer, J.P., Xu, H., and Raper, J.A. (2007). The detection and quantification of growth cone collapsing activities. Nat. Protoc. *2*, 2005–2011.

Meijering, E., Jacob, M., Sarria, J.C., Steiner, P., Hirling, H., and Unser, M. (2004). Design and validation of a tool for neurite tracing and analysis in fluorescence microscopy images. Cytometry A *58*, 167–176.

Parrinello, S., Noon, L.A., Harrisingh, M.C., Digby, P.W., Rosenberg, L.H., Cremona, C.A., Echave, P., Flanagan, A.M., Parada, L.F., and Lloyd, A.C. (2008). NF1 loss disrupts Schwann cell-axonal interactions: a novel role for semaphorin 4F. Genes Dev. *22*, 3335–3348.

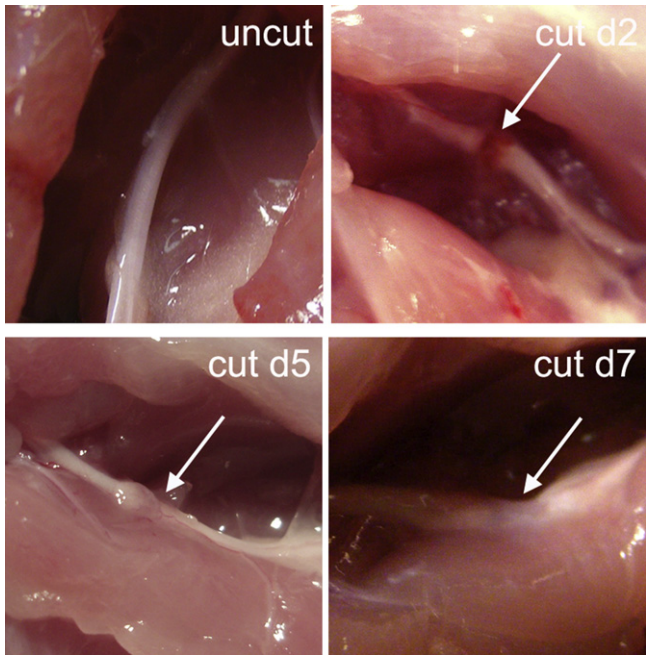

Figure S1. Rat Sciatic Nerves Reconnect Spontaneously after Full Transection, Related to Figure 1
Photographs of rat sciatic nerves prior (uncut) or following transection at the indicated days post-surgery.

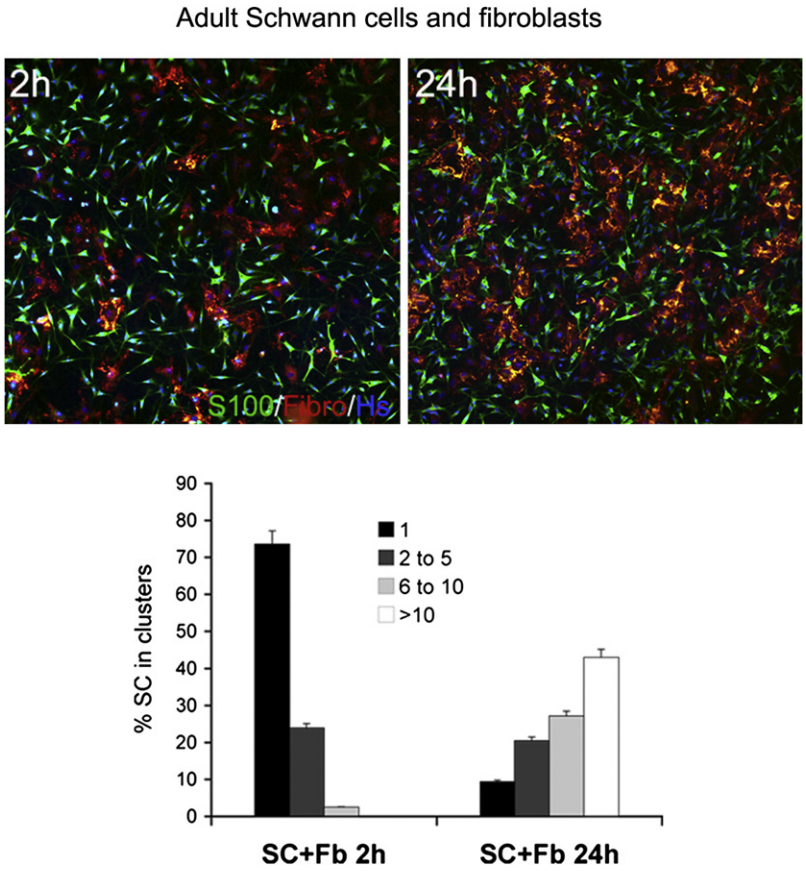

Figure S2. Adult Schwann Cell and Nerve Fibroblasts Undergo Cell Sorting in Culture, Related to Figure 2

Representative images and quantifications of primary Schwann cell/fibroblast co-cultures at 2 and 24 hr after seeding. Cells were isolated from 6 week old rat sciatic nerves and stained for S100β and fibronectin. Data are represented as mean ± SD.

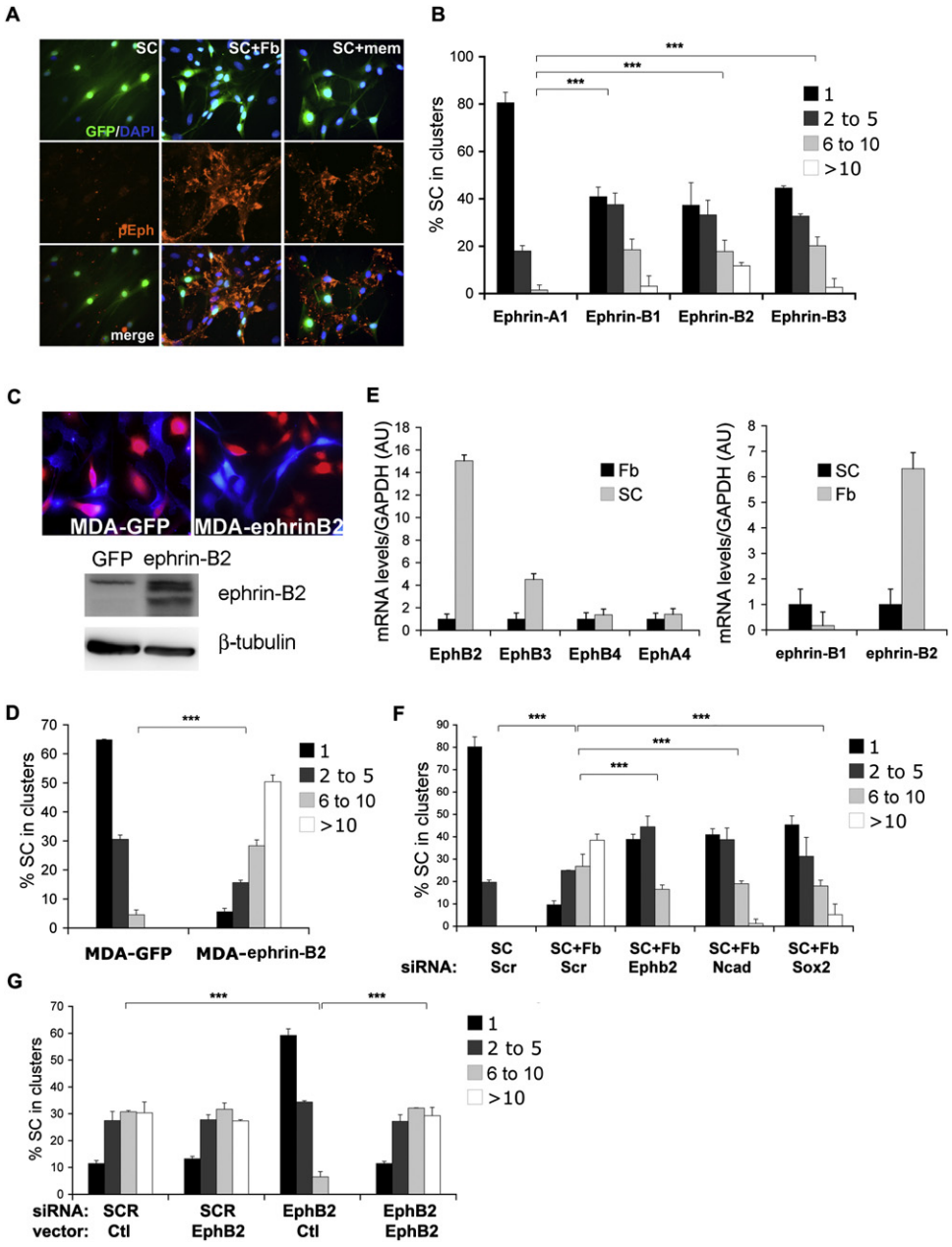

Figure S3. Ephrin-B/EphB Signaling Directs Schwann Cell Sorting in the Presence of Fibroblasts, Related to Figure 3

(A) Immunofluorescence analysis of phosphorylated Eph receptor (red) of GFP-labeled Schwann cells cultured on their own (SC), with fibroblasts (SC+Fb) or on fibroblast membranes (SC+mem) for 24 hr. Nuclei are counterstained with Hoechst.

(B) Quantification of clustering in Schwann cell monocultures treated with the indicated recombinant preclustered ephrin ligands for 24h. Shown is one experiment of three that gave similar results. Data for ephrin A1 stimulation are representative of all A ligands tested which had no clustering effect.

(C) Representative images of Schwann cells (blue) co-cultured with MDA-MB-435 breast cancer cells (red) engineered to express GFP (MDA- GFP) or ephrin-B2 (MDA- ephrinB2) and Western blots showing ectopic ephrin-B2 expression and β-tubulin as loading control.

(D) Quantification of Schwann cell clustering for experiment described in C.

(E) Quantitative RT-PCR analysis of relative expression levels of EphB receptors (left panel) and ephrin-B ligands (right panel) in Schwann cells and fibroblast monocultures as indicated. Bars represent average expression levels of three independent experiments. Error bars represent SEM.

(F) Quantification of clustering of scr siRNA-treated Schwann cells in the absence (SC Scr) or presence of fibroblasts (SC+Fb Scr) and EphB2, N-cadherin and Sox2 knock-down Schwann cells cultured in the presence of fibroblasts (SC+Fb N-cad) using a second independent siRNA oligo.

(G) Quantification of clustering of scr- or EphB2-siRNA treated rat Schwann cells co-cultured with fibroblasts and transfected with a control plasmid or a plasmid encoding mouse EphB2.

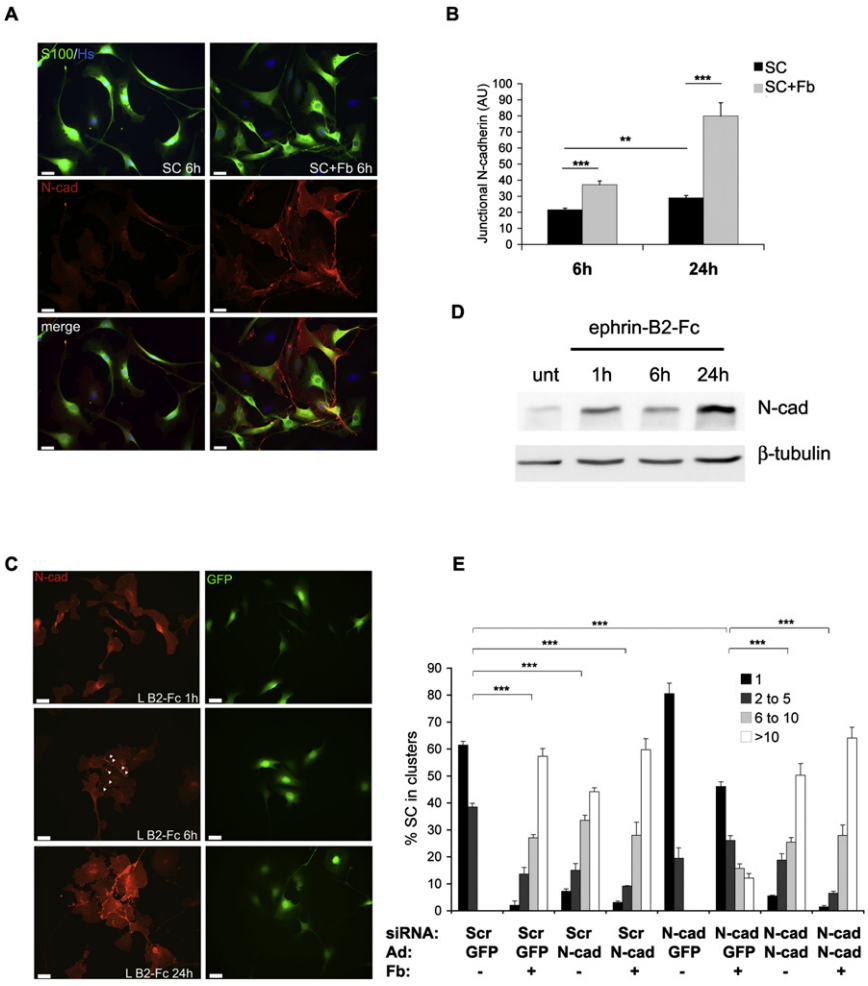

Figure S4. Sorting Results from the Rapid Relocalization of N-Cadherin to Cell Junctions upon Ephrin-B Stimulation, Related to Figure 5

(A) Immunofluorescence analysis for N-cadherin and S100β of Schwann cells cultured on their own or with fibroblasts for 6h. Nuclei are counterstained with Hoechst. Scale bar = 25 μm.

(B) Quantification of N-cadherin fluorescence at cell-cell contacts in Schwann cell cultured alone (SC) or in the presence of fibroblasts (SC+Fb) for 6 or 24h. Bars represent average pixel intensity normalized to junction area. Error bars depict SEM.

(C) Immunofluorescence analysis for N-cadherin of GFP-labeled Schwann cells treated with pre-clustered ephrin-B2-Fc for the indicated time intervals. Scale bar = 25 μm.

(D) Western blot analysis of N-cadherin expression in total protein lysates from Schwann cells treated as in C. β-tubulin was used as loading control.

(E) Quantification of clustering of scr- or N-cad-siRNA treated Schwann cells infected with GFP or siRNA-insensitive N-cadherin adenoviral vectors and cultured in the absence (-) or presence (+) of fibroblasts.

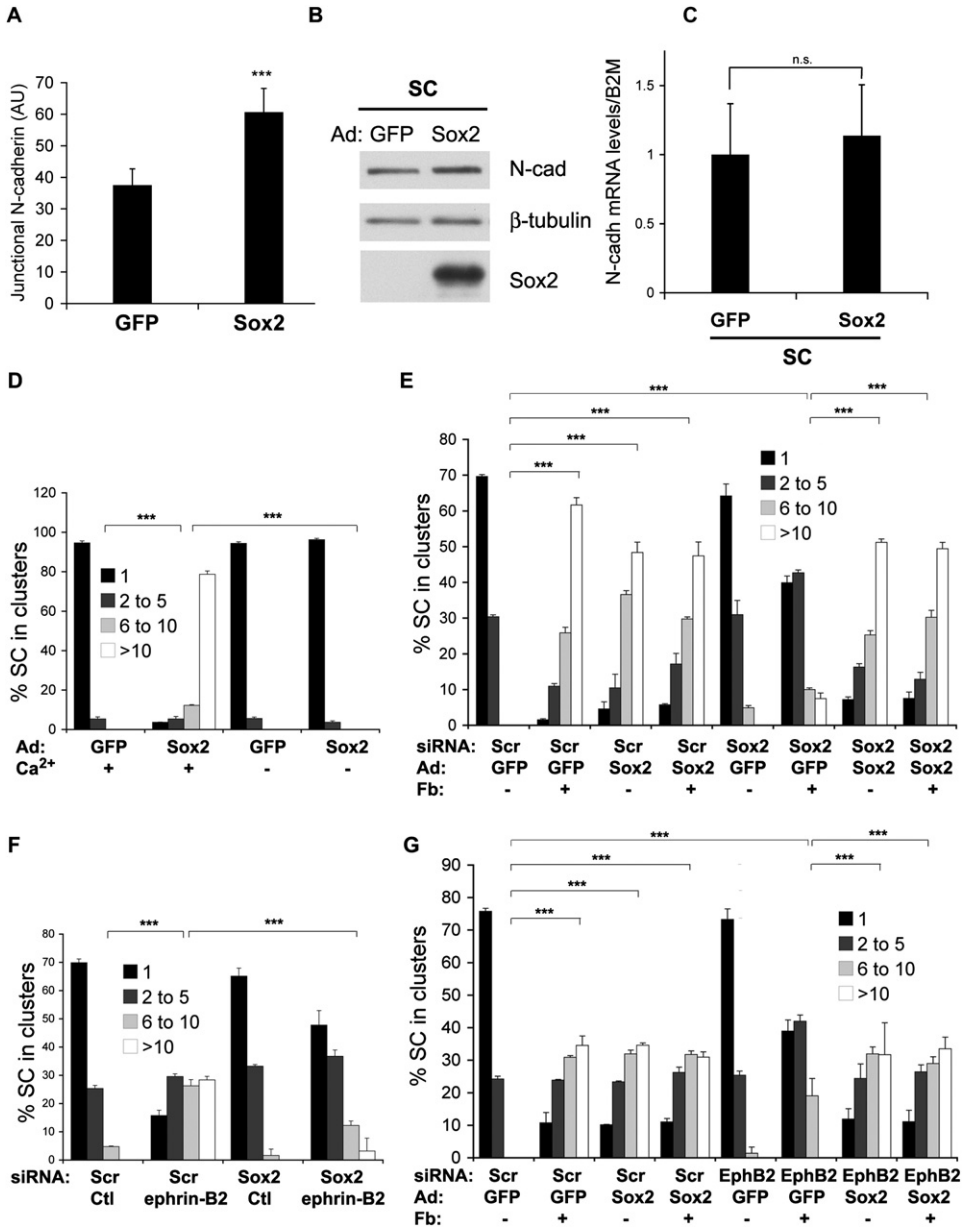

Figure S5. Sox2 Does Not Induce the Transcription of N-Cadherin, Related to Figure 6

(A) Quantification of N-cadherin staining at junctions in GFP and Sox2 overexpressing cells. Average pixel intensity at cell-cell contacts is shown. Error bars represent SEM.

(B) Western analysis of N-cadherin, β-tubulin and Sox2 levels in lysates of Schwann cell cultures overexpressing GFP or Sox2.

(C) Quantitative RT-PCR analysis of N-cadherin mRNA levels in Schwann cells engineered to overexpress GFP or Sox2. Shown is the average expression of three independent experiments normalized to GAPDH. Error bars depict SEM across experiments.

(D) Quantification of clustering of Schwann cell cultures infected with GFP or Sox2 adenoviral vectors and cultured in normal (+) or low Ca^{2+} (-) media.

(E) Quantification of clustering of scr- or Sox2-siRNA treated Schwann cells infected with adenoviral vectors encoding GFP or siRNA-insensitive mouse Sox2 and cultured in the absence (-) or presence (+) of fibroblasts.

(F) Quantification of clustering of Schwann cells transfected with scr- or Sox2-siRNA and treated with control proteins or ephrin-B2-Fc.

(G) Quantification of clustering of scr- or EphB2-siRNA treated Schwann cells infected with GFP or Sox2 adenoviral vectors and cultured in the absence (-) or presence (+) of fibroblasts.

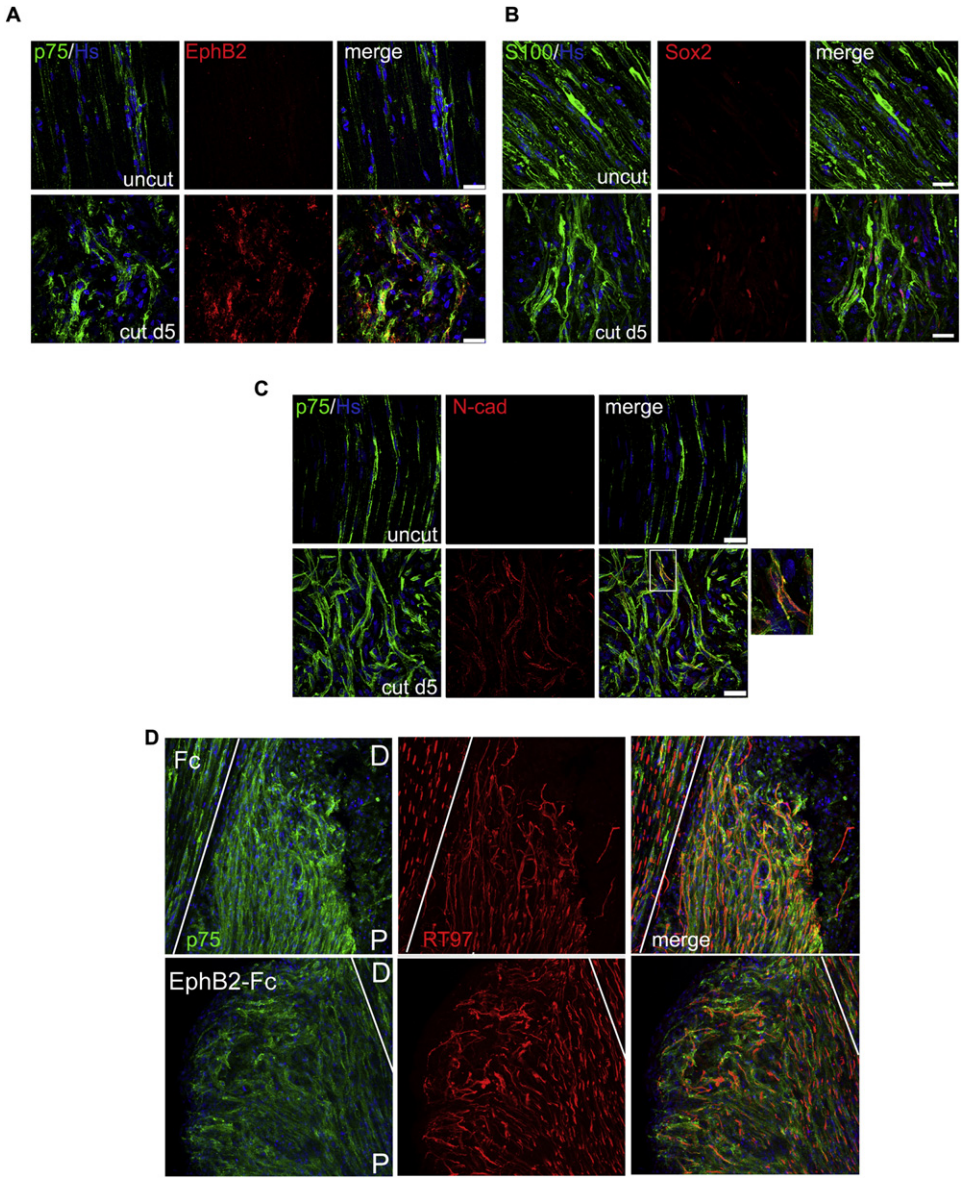

Figure S6. Schwann Cell Cords in the Nerve Bridge Express EphB2, N-Cadherin and Sox2, Related to Figure 7

(A–C) Immunofluorescence staining of sections of contralateral (uncut) and nerve bridges 5 days post transection (cut d5) for the indicated proteins. S100β and p75NGFR were used to co-stain Schwann cells. Nuclei were counterstained with Hoechst. Scale bar = 25 μm.

(D) Immunofluorescence analysis for Schwann cell and axonal markers p75NGFR and RT97. Shown are representative sections of proximal stumps of half-cut nerves exposed to Fc controls or EphB2-Fc inhibitor proteins for 4 days. Note the almost complete co-localization of regrowing axons and migrating Schwann cells (merge).